processes. This is especially true in the energy and angular region studied in Ref. 6.

One interesting question about the Nemets effect concerns its sign. One might think that closed-shell nuclei should have a less-diffuse surface than their neighbors and therefore a smaller breakup cross section, contrary to the experimental result. However, Goldhaber[13] has pointed out that a diffuse surface would be a more efficient absorber of nucleons, a process which competes with simple breakup. On the other hand, there is no evidence that cross sections for nucleon absorption processes like (d, p) or (d, n) vary between closed-shell and neighboring nuclei.

[13] M. Goldhaber (private communication).

PHYSICAL REVIEW VOLUME 185, NUMBER 4 20 SEPTEMBER 1969

Giant Resonance in Deformed Nuclei: Photoneutron Cross Sections for Eu^{153}, Gd^{160}, Ho^{165}, and W^{186}†

B. L. BERMAN, M. A. KELLY,* R. L. BRAMBLETT,‡ J. T. CALDWELL, H. S. DAVIS, AND S. C. FULTZ

Lawrence Radiation Laboratory, University of California, Livermore, California 94550

(Received 17 February 1969)

Photoneutron cross sections, including $\sigma[(\gamma, n)+(\gamma, pn)]$, $\sigma[(\gamma, 2n)+(\gamma, p2n)]$, and $\sigma(\gamma, 3n)$, were measured for Eu^{153}, Gd^{160}, Ho^{165}, and W^{186} as a function of photon energy from 8 to 29 MeV. The photon energy resolution varied from less than 300 keV at the lowest to 400 keV at the highest energies, and the data were taken at intervals of 300 keV or less. The source of radiation was the monoenergetic photon beam obtained from the annihilation in flight of fast positrons. The partial cross sections were determined by neutron multiplicity counting, and the average neutron energies for both single- and double-photoneutron events were determined simultaneously with the cross-section data by the ring-ratio technique. Nuclear information extracted from the data includes giant-resonance parameters, integrated cross sections and their moments, nuclear symmetry energies, intrinsic quadrupole moments, and nuclear level density parameters. The data were analyzed to obtain a mean radius parameter $R_0=1.26\pm0.02$ F for these nuclei.

I. INTRODUCTION

THE study of the giant electric dipole resonance in statically deformed nuclei provides both a sensitive test of the classical hydrodynamic model of the nucleus[1,2] and a means of obtaining several important parameters which describe the properties of such nuclei, notably their shape. The hydrodynamic theory, as applied to deformed nuclei,[3–5] makes two major predictions which lend themselves particularly to experimental scrutiny: (1) that the giant resonance is split into two components for spheroidal nuclei, corresponding to dipole vibrations, along the major and minor axes of the spheroid, of two interpenetrating fluids made up of the neutrons and protons in the nucleus; and (2) that the strengths of these two components have the simple ratio of 1:2, corresponding to the number of degrees of freedom for these vibrations. The first condition gives a prescription for the nuclear shape parameters for prolate nuclei, by means of the relation

$$E_m(2)/E_m(1)=0.911\eta+0.089, \quad (1)$$

where $E_m(1)$ and $E_m(2)$ are the lower and higher resonance energies of the two components of the giant resonance and η is the nuclear deformation parameter which is the ratio of the major to the minor axis. The intrinsic quadrupole moment Q_0 for the nucleus then can be computed from the expression

$$Q_0=\tfrac{2}{5}ZR^2(\eta^2-1)\eta^{-2/3}=\tfrac{2}{5}ZR^2\epsilon, \quad (2)$$

where the nuclear radius $R=R_0A^{1/3}$, Z and A are the atomic number and atomic weight, respectively, and the parameter ϵ is the nuclear eccentricity (see Sec. IV). It should be pointed out that while the Coulomb-excitation method for obtaining the quadrupole moment depends upon the transition probability $B(E2)$ according to the formula

$$Q_0^2=(16\pi/5)B(E2) \quad (3)$$

(for even-even nuclei) and hence gives only the magnitude of Q_0, the photonuclear method gives its

† Work performed under the auspices of the U.S. Atomic Energy Commission; a preliminary account of this work appears in Bull. Am. Phys. Soc. **14**, 103 (1969).

* Now at Hewlett-Packard Corp., Palo Alto, Calif.

‡ Now at Gulf General Atomic Inc., San Diego, Calif.

[1] M. Goldhaber and E. Teller, Phys. Rev. **74**, 1046 (1948).

[2] H. Steinwedel and J. H. D. Jensen, Z. Naturforsch. **5a**, 413 (1950).

[3] K. Okamoto, Progr. Theoret. Phys. **15**, 75L (1956).

[4] M. Danos, Nucl. Phys. **5**, 23 (1958).

[5] K. Okamoto, Phys. Rev. **110**, 143 (1958).

sign as well. The second condition above predicts that the ratio of the area under the lower energy component of the giant resonance to that under the upper energy component be $\frac{1}{2}$ for prolate nuclei but 2 for oblate nuclei, since the mode of vibration along the long axis of the nucleus has the lower frequency and hence the lower energy, and vice versa. This area ratio R_A is given by

$$R_A=\sigma_m(1)\,\Gamma(1)/\sigma_m(2)\,\Gamma(2), \qquad (4)$$

where $\sigma_m(1)$ and $\sigma_m(2)$ are the peak cross sections for the lower and upper components, respectively,and $\Gamma(1)$ and $\Gamma(2)$ are their widths. In addition, the photonuclear experiments provide the information necessary to compute the nuclear symmetry energy K: For prolate deformed nuclei, K is obtained from the relation

$$K=9.935\times10^{-4}\frac{A^{8/3}}{NZ}\frac{[E_m(1)]^2}{1-[\Gamma(1)/2E_m(1)]^2}\times\frac{\eta^{4/3}}{(1+0.01860\epsilon-0.03314\epsilon^2)^2}. \qquad (5)$$

Several experiments have been reported previously[6] which have confirmed qualitatively the above two basic predictions of the hydrodynamic model. However, a more recent experiment performed at this Laboratory by Kelly *et al.*[7] (also see Ref. 8), while it confirmed definitely the underlying assumption of the hydrodynamic theory that the two peaks in the giant resonance are associated with the absorption of photons polarized along the major and minor axes of the nucleus, has shown there to be a quantitative discrepancy between the experimental data and the prediction of that theory, even when it is modified to account for the coupling of surface modes of vibration with the electric dipole photon absorption.[9] By aligning their target sample of Ho^{165} nuclei both parallel to and perpendicular to the incoming photon beam and then measuring the total photoneutron cross section in the giant-resonance region for each case (as well as for the unaligned case), Kelly *et al.*[7] have shown that the total asymmetry of the giant-resonance splitting is about 25% smaller (and at least two standard deviations from zero) than that predicted by either theory.

Since such experiments with polarized targets are extremely difficult, however, it is necessary to make use of another approach in order to test further in a quantitative way the theoretical predictions. One such approach is to perform a systematic survey of nuclei in the deformed rare-earth region of the periodic table, both (1) comprehensive enough to delineate the systematics of such deviations from the theoretical predictions as may exist, and in particular of the area ratio R_A, and (2) precise enough to determine unambiguously and within reasonable experimental limits the deformation parameters, quadrupole moments, nuclear symmetry energies, and nuclear level densities of the specific nuclei studied so that they can be compared with the results of other measurements. The measurements reported here on the four nuclei Eu^{153}, Gd^{160}, Ho^{165}, and W^{186}, which span the region of deformed nuclei, were undertaken in a continuing series of experiments on the giant resonance by the photonuclear group at the Livermore electron linear accelerator in order to provide, together with the results of earlier work performed at this Laboratory on Tb^{159} [10] and Ta^{181},[11] the elements of such a survey. The results on Ho^{165} reported here supersede the earlier work on that nucleus given in Ref. 11.

Most earlier photoneutron measurements on Gd^{160},[12] W^{186},[13] and Ho^{165},[6,14–16] and indeed throughout the region of deformed rare-earth nuclei in the range of photon energies corresponding to the giant-resonance region, have been made with bremsstrahlung as the source of radiation. This does not include the Livermore work referred to above[7,10,11] nor the work on Ho^{165} of Axel *et al.*[17] Also, there have been no such measurements on Eu^{153} reported heretofore. The measurements with bremsstrahlung sources have been accompanied by all the difficulties attendant upon the unfolding of the resultant yield curves and have not made use of neutron-multiplicity counting, which resulted in no firm knowledge being obtained of the partial, and hence total, cross sections above the $(\gamma, 2n)$ threshold. This latter point is particularly important in heavy nuclei such as these since the $(\gamma, 2n)$ threshold always occurs in or below the second giant-resonance peak, and thus these earlier results cannot provide the unambiguous values for the giant-resonance parameters necessary to test the theoretical predictions quantitatively.

The present measurements were made with the monoenergetic photon beam obtained from the annihilation in flight of fast positrons as the source of radiation, and with the use of an efficient paraffin-and-BF_3-tube 4π neutron detector for neutron-multiplicity counting. They provide independent, simultaneous

[6] Beginning with E. G. Fuller, B. Petree, and M. S. Weiss, Phys. Rev. **112**, 554 (1958).
[7] M. A. Kelly, B. L. Berman, R. L. Bramblett, and S. C. Fultz, Phys. Rev. **179**, 1194 (1969).
[8] E. Ambler, E. G. Fuller, and H. Marshak, Phys. Rev. **138**, B117 (1965).
[9] M. Danos and W. Greiner, Phys. Rev. **134**, B284 (1964).
[10] R. L. Bramblett, J. T. Caldwell, R. R. Harvey, and S. C. Fultz, Phys. Rev. **133**, B869 (1964).
[11] R. L. Bramblett, J. T. Caldwell, G. F. Auchampaugh, and S. C. Fultz, Phys. Rev. **129**, 2723 (1963).
[12] J. H. Carver and W. Turchinetz, Proc. Phys. Soc. (London) **73**, 69 (1959).
[13] J. H. Carver, D. C. Peaslee, and R. B. Taylor, Phys. Rev. **127**, 2198 (1962).
[14] L. Katz and G. B. Chidley, *Nuclear Reactions at Low and Medium Energies* (Academy of Sciences, USSR, 1958), p. 371.
[15] H. H. Thies and B. M. Spicer, Australian J. Phys. **13**, 505 (1960).
[16] E. G. Fuller and E. Hayward, Nucl. Phys. **30**, 613 (1962).
[17] P. Axel, J. Miller, C. Schuhl, G. Tamas, and C. Tzara, J. Phys. (Paris) **27**, 262 (1966).

TABLE I. Sample specifications.

Nucleus	Mass (g)	Chemical form	Purity (%)	Principal impurities (%)	
Eu^{153}	100.1	Oxide	98.8	Eu^{151}	1.2
Gd^{160}	46.0	Oxide	97.9	Gd^{158}	0.9
				Gd^{157}	0.5
				$Gd^{155,156}$	0.3 each
Ho^{165}	191.5	Metal	≥99.9	Negligible	
W^{186}	79.6	Oxide	97.2	W^{184}	2.0
				W^{182}	0.4
				W^{183}	0.3

determinations of the partial photoneutron cross sections necessary to ascertain the true shape of the giant resonance for these nuclei. They also allow one to extract Lorentz parameters, integrated cross sections and their moments, average photoneutron energies, nuclear symmetry energies, intrinsic quadrupole moments and other shape parameters, and nuclear level density and shell-plus-pairing-effect parameters.

II. EXPERIMENTAL DETAILS

The main features of the experimental techniques have been given in previous papers,[18,19] including the ring-ratio technique,[18–22] whereby the average energy of the photoejected neutrons for both single- and double-photoneutron events is determined for each data point. These energies not only are of interest in themselves, but also serve to determine the neutron detector efficiencies necessary to compute both the single- and double-photoneutron cross sections, $\sigma[(\gamma, n)+(\gamma, pn)]$ and $\sigma[(\gamma, 2n)+(\gamma, p2n)]$, respectively. Triple-photoneutron events were assumed to follow the same efficiency curves as double-photoneutron events, except for the displacement of the threshold energies; the errors introduced into the total photoneutron cross sections $\sigma[(\gamma, n)+(\gamma, pn)+(\gamma, 2n)+(\gamma, p2n)+(\gamma, 3n)]$ by this procedure were judged to be negligible, even when the triple-photoneutron cross sections $\sigma(\gamma, 3n)$ themselves are not small, because of the predominantly statistical nature of multiple-neutron emission. The differences between the present measurements and the earlier Livermore work[10,11] stem largely from the use of the present 40% efficient neutron detector (the older detector was only half as efficient), which makes possible the collection of much better $(\gamma, 2n)$ and $(\gamma, 3n)$ data as well as the use of the ring-ratio technique. As a consequence, the present absolute cross sections have been determined with an uncertainty of at most 7% (as compared with 10% for the earlier data). The relative precision of the cross-section measurements between different nuclei, however, is far better (2–3%).

The photon energy resolution for the present measurements varied from less than 300 keV at 10 MeV to 400 keV at 30 MeV, which corresponds to the use of a 0.030-in.-thick Be annihilation target.[23] The absolute energy scale is known to within 0.25%.

The sample specifications are given in Table I. Although holmium is monoisotopic, the other three elements studied are not, and, therefore, highly enriched, separated isotopic samples were used. This fact also is important here, since the presence of contaminants of other isotopes would introduce serious uncertainties in the interpretation of the data, not only because the contaminants would have different giant-resonance parameters, but also because the widely varying $(\gamma, 2n)$ thresholds would make an unambiguous measurement of the partial cross sections extremely difficult.

Corrections to the data, to compensate for the attenuation of the photon beam in passing through the samples, introduced no more than 0.5% uncertainty in the cross-section values. The Eu_2O_3, Gd_2O_3, and WO_3 samples were contained in thin-walled Lucite cylinders, for which the appropriate sample blank subtractions were made. The subtraction of the effect of the oxygen in the samples was done with the aid of the photoneutron

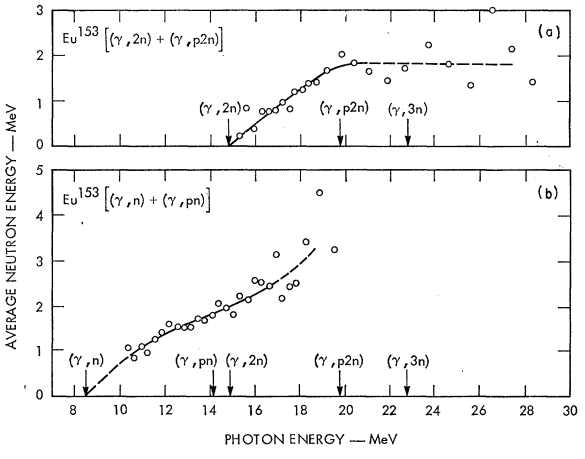

FIG. 1. Average neutron energies for Eu^{153} derived from the ring-ratio data and plotted as functions of photon energy (see text): (a) for $[(\gamma, 2n)+(\gamma, p2n)]$ events, (b) for $[(\gamma, n)+(\gamma, pn)]$ events. The thresholds (arrows) are from Ref. 24.

[18] B. L. Berman, J. T. Caldwell, R. R. Harvey, M. A. Kelly, R. L. Bramblett, and S. C. Fultz, Phys. Rev. **162**, 1098 (1967), and references therein.

[19] B. L. Berman, R. L. Bramblett, J. T. Caldwell, H. S. Davis, M. A. Kelly, and S. C. Fultz, Phys. Rev. **177**, 1745 (1969).

[20] B. L. Berman, R. L. Bramblett, J. T. Caldwell, R. R. Harvey, and S. C. Fultz, Phys. Rev. Letters **15**, 727 (1965).

[21] J. T. Caldwell, R. L. Bramblett, B. L. Berman, R. R. Harvey, and S. C. Fultz, Phys. Rev. Letters **15**, 976 (1965).

[22] S. C. Fultz, J. T. Caldwell, B. L. Berman, R. L. Bramblett, and R. R. Harvey, Phys. Rev. **143**, 790 (1966).

[23] R. L. Bramblett, J. T. Caldwell, B. L. Berman, R. R. Harvey, and S. C. Fultz, Phys. Rev. **148**, 1198 (1966).

TABLE II. Photoneutron threshold values.[a]

Nucleus	$E_{thr}(\gamma, n)$	$E_{thr}(\gamma, pn)$	$E_{thr}(\gamma, 2n)$	$E_{thr}(\gamma, p2n)$	$E_{thr}(\gamma, 3n)$
Eu^{153}	8.54±0.01	14.13±0.02	14.83±0.02	19.74±0.02	22.77±0.02
Gd^{160}	7.38±0.03	16.1±0.3	13.41±0.01	21.83±0.05	21.34±0.01
Ho^{165}	8.04±0.04	13.81±0.02	14.60±0.02	20.06±0.02	23.00±0.04
W^{186}	7.21±0.04	14.9±0.1	12.96±0.04	20.67±0.05	20.38±0.05

[a] From Ref. 24. All quantities in this table are given in MeV.

cross section for oxygen measured previously at this Laboratory.[10,21] These combined corrections were negligible (<0.3%) in the giant-resonance region, although they totaled 36, 44, and 54% of the total photoneutron cross sections for Eu^{153}, Gd^{160}, and W^{186}, respectively, at 22.3 MeV, the highest peak in the giant resonance of O^{16}.

The threshold values for the various photoneutron reactions are given in Table II, and are shown in the plots by arrows. The threshold energies determined in the present measurements all agree, within the experimental limits, with the values tabulated in Mattauch *et al.*[24]

III. RESULTS

A. Average Photoneutron Energies

The average neutron energies $\bar{E}_n$ for $(\gamma, n)+(\gamma, pn)$ and $(\gamma, 2n)+(\gamma, p2n)$ events for Eu^{153}, Gd^{160}, Ho^{165}, and W^{186} derived from the ring-ratio data mentioned above are shown as functions of photon energy in Figs. 1–4, respectively. The relatively poor statistics are perhaps best indicated by the scatter of the data points; curves were drawn only where the data were judged to justify such a procedure. Table III gives the values for $\bar{E}_n(1)$, the average neutron energy for $(\gamma, n)+(\gamma, pn)$ events, both at the lower peak of the giant resonance and at the $(\gamma, 2n)$ threshold. Also given are values for $\bar{E}_n(2)$, the average neutron energy for $(\gamma, 2n)+(\gamma, p2n)$ events, both at the highest point in the $(\gamma, 2n)+(\gamma, p2n)$ cross section and at high photon energies [greater than 3–5 MeV above the $(\gamma, 2n)$ threshold], where $\bar{E}_n(2)$ apparently approaches an asymptotic value. While the first and third quantities fall into no obvious pattern, the other two seem to be characteristic of the nucleus, and perhaps can be said to decrease with increasing neutron number. Insofar as the average neutron energy for (γ, n) events far above the (γ, n) threshold, as represented by $\bar{E}_n(1)|_{(\gamma,2n)}$, and the average energy for the *first* neutron emitted in $(\gamma, 2n)$ events far above the $(\gamma, 2n)$ threshold, which is related to, but somewhat higher than $\bar{E}_n(2)|_{asymp}$, are the same, the nuclear temperature of the target-minus-one-neutron nucleus is constant. The values for these two quantities in Table III support this point of view. The fact that in all cases $\bar{E}_n(1)$ continues to rise rapidly above the $(\gamma, 2n)$ threshold can be understood as simply owing to the opening of the $(\gamma, 2n)$ decay channel, which bleeds off the events characterized by low-energy photoneutrons. The sharp dip in $\bar{E}_n(1)$ for Gd^{160} seems to be associated with the (γ, pn) threshold, which in this case is well separated from the $(\gamma, 2n)$ threshold. The dip, then, might be attributed to the growth of the (γ, pn) reaction, which will contribute low-energy neturons to the single-photoneturon events owing to the large

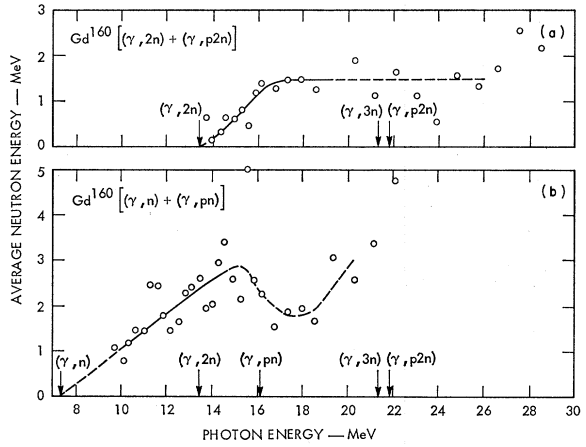

FIG. 2. Average neutron energies for Gd^{160}: (a) for $[(\gamma, 2n)+(\gamma, p2n)]$ events, (b) for $[(\gamma, n)+(\gamma, pn)]$ events.

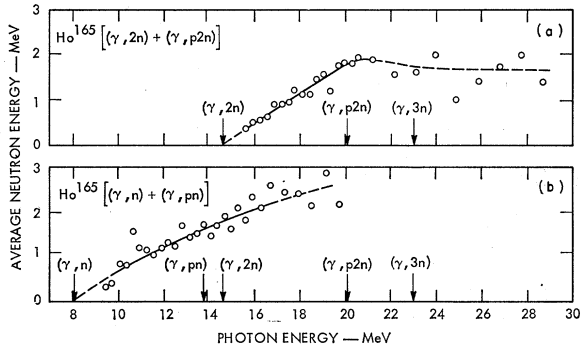

FIG. 3. Average neutron energies for Ho^{165}: (a) for $[(\gamma, 2n)+(\gamma, p2n)]$ events, (b) for $[(\gamma, n)+(\gamma, pn)]$ events.

[24] J. H. E. Mattauch, W. Thiele, and A. H. Wapstra, Nucl. Phys. **67**, 32 (1965).

TABLE III. Average neutron energies.[a]

Nucleus	$E_m(1)$	$\bar{E}_n(1)\|_m$ [b]	$\bar{E}_n(1)\|_{(\gamma,2n)}$ [c]	$E_m(\gamma, 2n)$	$\bar{E}_n(2)\|_m$ [d]	$\bar{E}_n(2)\|_{asymp}$ [e]
Eu^{153}	12.33	1.4	2.0	17.6	1.1	1.8
Gd^{160}	12.23	1.9	2.3	16.2	1.3	1.5
Ho^{165}	12.28	1.3	1.8	16.9	0.8	1.7
W^{186}	12.58	1.4	1.6	15.7	1.2	1.3

[a] All quantities in this table are given in MeV.
[b] Average neutron energy at $E_\gamma = E_m(1)$, the energy of the lower peak of the giant resonance.
[c] Average neutron energy at $E_\gamma = E_{thr}(\gamma, 2n)$.
[d] Average neutron energy for $(\gamma, 2n)$ neutrons alone at $E_\gamma = E_m(\gamma, 2n)$, the energy where $\sigma(\gamma, 2n)$ is a maximum.
[e] Average neutron energy for $(\gamma, 2n)+(\gamma, p2n)$ neutrons for photon energies greater than 3–5 MeV above $E_{thr}(\gamma, 2n)$.

Coulomb barrier for protons. There is a suggestion of this effect in the W^{186} data also where the thresholds are again well separated; but the statistical limitations of both the Gd^{160} ring-ratio data (it was the smallest sample of those studied here) and also the W^{186} ring-ratio data preclude any more serious consideration of this effect at present.

B. Cross Sections

The photoneutron cross sections for Eu^{153}, Gd^{160}, Ho^{165}, and W^{186} are shown as functions of photon energy in Figs. 5–8, respectively. Since the main emphasis of this work was to explore the systematics of the giant resonance rather than to attempt a detailed measurement of its fine structure, the data points were spaced rather widely (every 310 keV, except for several more closely spaced points in the giant-resonance peak in Gd^{160} and in W^{186}) and the photon energy resolution was chosen to be comparable with this spacing (see Sec. II). It should be noted, however, that this spacing still is narrower than the typical 0.5- or 1.0-MeV unfolding intervals for bremsstrahlung experiments, and also that any structure which is wider than ~600 keV will be delineated clearly in the present data.

1. Eu^{153}

The total photoneutron cross section for Eu^{153} [Fig. 5(a)] exhibits clearly the splitting of the giant resonance into two components characteristic of deformed nuclei, even though its neutron number ($N=90$) barely places it in the region of deformed rare-earth nuclei. It is also evident that the higher-energy component has much the greater area, indicating that the nucleus is prolate. There is a peak in the cross section at 9.7 MeV, and less definite evidence for structure at several energies above the giant resonance, at 17 MeV and between 22 and 29 MeV. (Hurst and Donahue[25] measured the Eu^{153} (γ, n) cross section at three discrete energies just above threshold with monoenergetic photons and an activation technique, and obtained results somewhat higher than but in reasonable agreement with those presented here.) The single-photoneutron cross section [Fig. 5(b)] decreases to very small values (in fact, consistent with zero) by 19 MeV, about 4 MeV above the $(\gamma, 2n)$ threshold. Similar behavior of the single-photoneutron cross section has been observed for nearly every other medium or heavy nucleus studied at this laboratory, including the other nuclei reported on at present. The dashed line on this and on the other plots of $\sigma[(\gamma, n)+(\gamma, pn)]$ corresponds to a 4% systematic uncertainty in the subtraction of the neutron counts hwich result from the positron bremsstrahlung, and is important only for the single-photoneutron cross section for energies above the giant resonance. More recent measurements,[26] however, have shown that this uncertainty is almost certainly an overestimate, and probably should be halved. The double-photoneutron cross section [Fig. 5(c)] rises sharply from threshold and reaches its maximum value of about 95 mb at 17.6 MeV. The present determination of the $(\gamma, 2n)$ threshold energy, as in all cases reported upon here, is in agreement within the experimental limits (≈100 keV), with the value tabulated in Ref. 24. The $(\gamma, 3n)$ cross section [Fig. 5(d)] appears to reach its maximum value of about 16 mb at about 27.7 MeV, although it is possible that it is still rising at the upper limit of the present

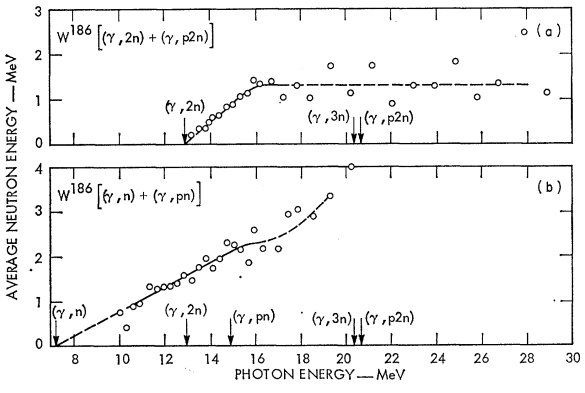

FIG. 4. Average neutron energies for W^{186}: (a) for $[(\gamma, 2n)+(\gamma, p2n)]$ events, (b) for $[(\gamma, n)+(\gamma, pn)]$ events.

[25] R. R. Hurst and D. J. Donahue, Nucl. Phys. **A91**, 369 (1967).

[26] B. L. Berman, M. A. Kelly, and S. C. Fultz (to be published).

measurement (29 MeV). Of course, if the total cross sections are to follow a Lorentz curve, the $(\gamma, 3n)$ cross sections must reach maxima and then begin to fall; the locations of these maxima, and also of the maxima for the $(\gamma, 2n)$ cross sections, might have implications for statistical theories. It has been observed for all of the medium and heavy nuclei studied at this laboratory, and in particular for the four cases presented here, that whereas the $(\gamma, 2n)$ cross sections always rise sharply from threshold (thus facilitating threshold determinations, and therefore determinations of the masses of

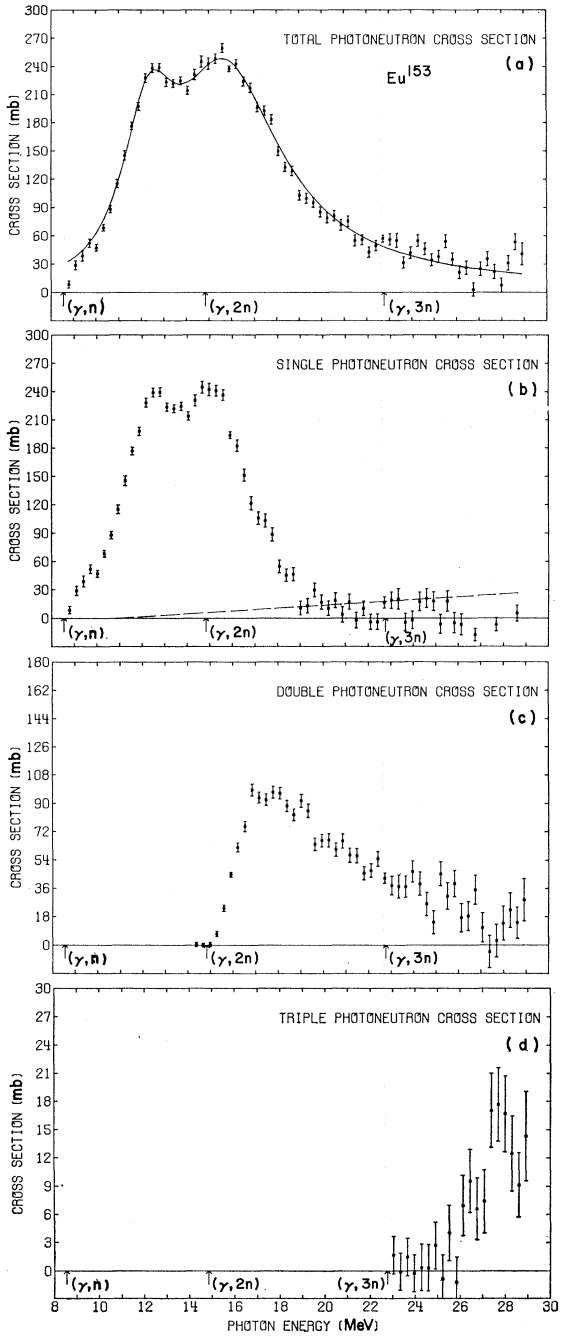

FIG. 5. Photoneutron cross sections for Eu^{153}. (a) Total photoneutron cross section $\sigma[(\gamma, n)+(\gamma, pn)+(\gamma, 2n)+(\gamma, p2n)+(\gamma, 3n)]$. The solid line is a two-component Lorentz-curve fit to the giant-resonance data (10.8–18.8 MeV). (b) Single-photoneutron cross section $\sigma[(\gamma, n)+(\gamma, pn)]$. The dashed line represents the maximum systematic error owing to the uncertainty in the normalization of the positron bremsstrahlung subtraction. (c) Double-photoneutron cross section $\sigma[(\gamma, 2n)+(\gamma, p2n)]$. (d) Triple photoneutron cross section $\sigma(\gamma, 3n)$.

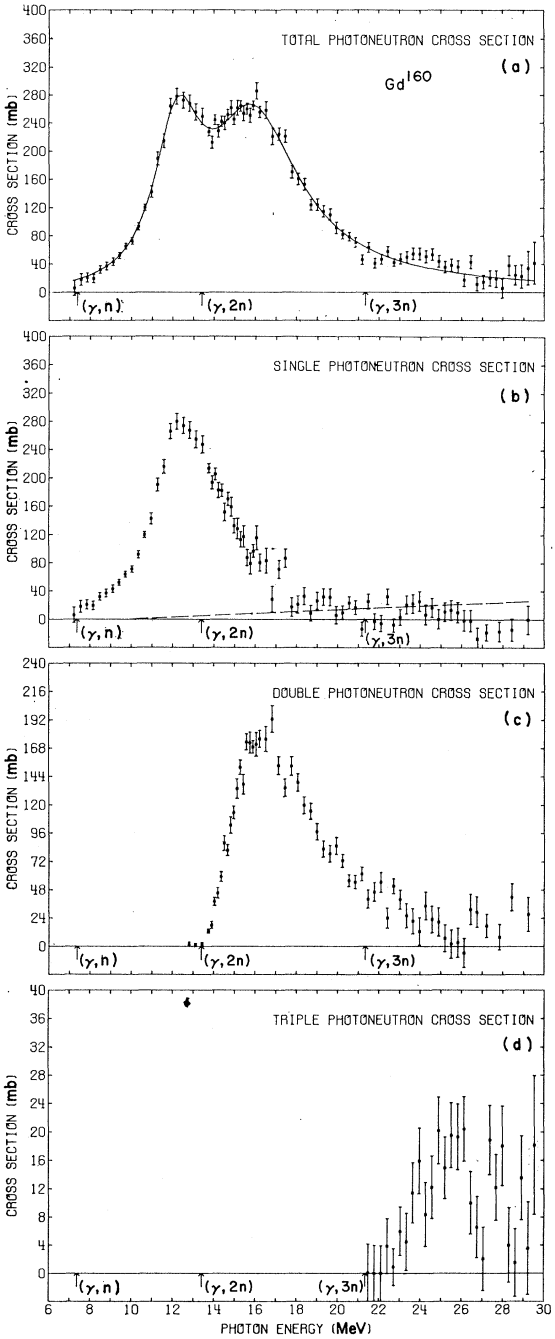

FIG. 6. Photoneutron cross sections for Gd^{160}: (a) $\sigma[(\gamma, n)+(\gamma, pn)+(\gamma, 2n)+(\gamma, p2n)+(\gamma, 3n)]$, (b) $\sigma[(\gamma, n)+(\gamma, pn)]$, (c) $\sigma[(\gamma, 2n)+(\gamma, p2n)]$ (d) $\sigma(\gamma, 3n)$.

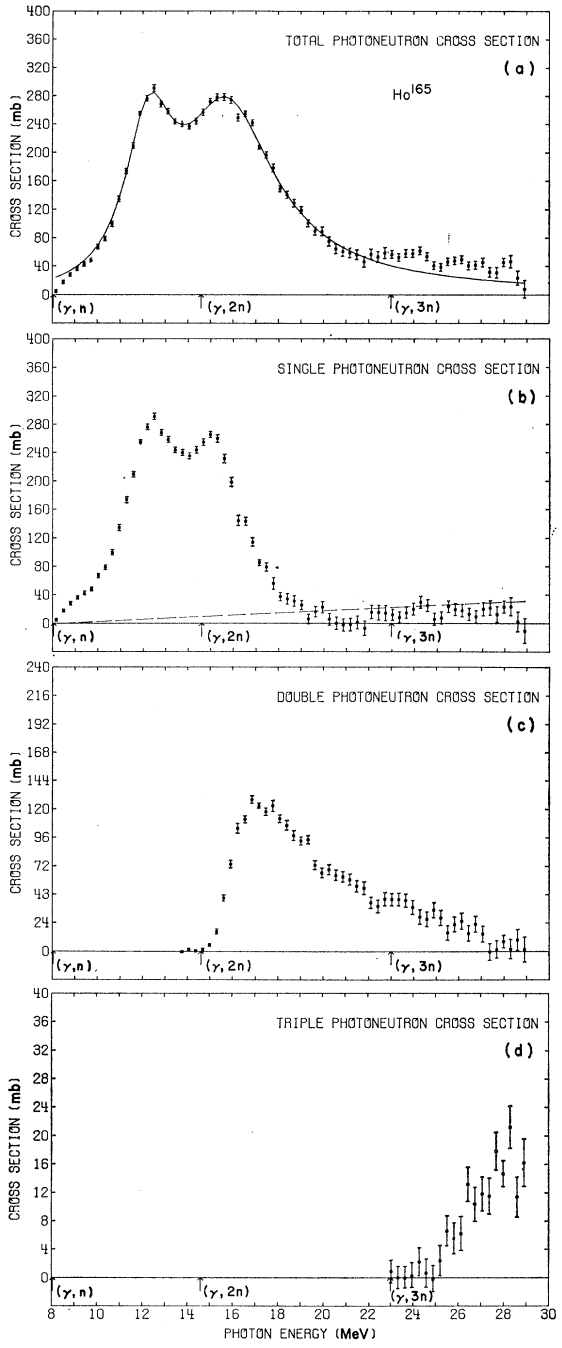

FIG. 7. Photoneutron cross sections for Ho^{165}: (a) $\sigma[(\gamma, n)+(\gamma, pn)+(\gamma, 2n)+(\gamma, p2n)+(\gamma, 3n)]$, (b) $\sigma[(\gamma, n)+(\gamma, pn)]$, (c) $\sigma[(\gamma, 2n)+(\gamma, p2n)]$, (d) $\sigma(\gamma, 3n)$.

target-minus-two-neutron nuclei[18,19]), the $(\gamma, 3n)$ cross sections always rise slowly and lead to threshold determinations in excess of the accepted values, where they are known.[18,19] For the present cases, this excess is about 2 MeV for Eu^{153} and Ho^{165}, and about 1 MeV for Gd^{160} and W^{186}.

2. Gd^{160}

The total photoneutron cross section for Gd^{160} [Fig. 6(a)] has the largest splitting between the two components of the giant resonance (3.7 MeV) of any nucleus yet measured, indicating that this mass number, or neutron number ($N=96$), is probably the midpoint

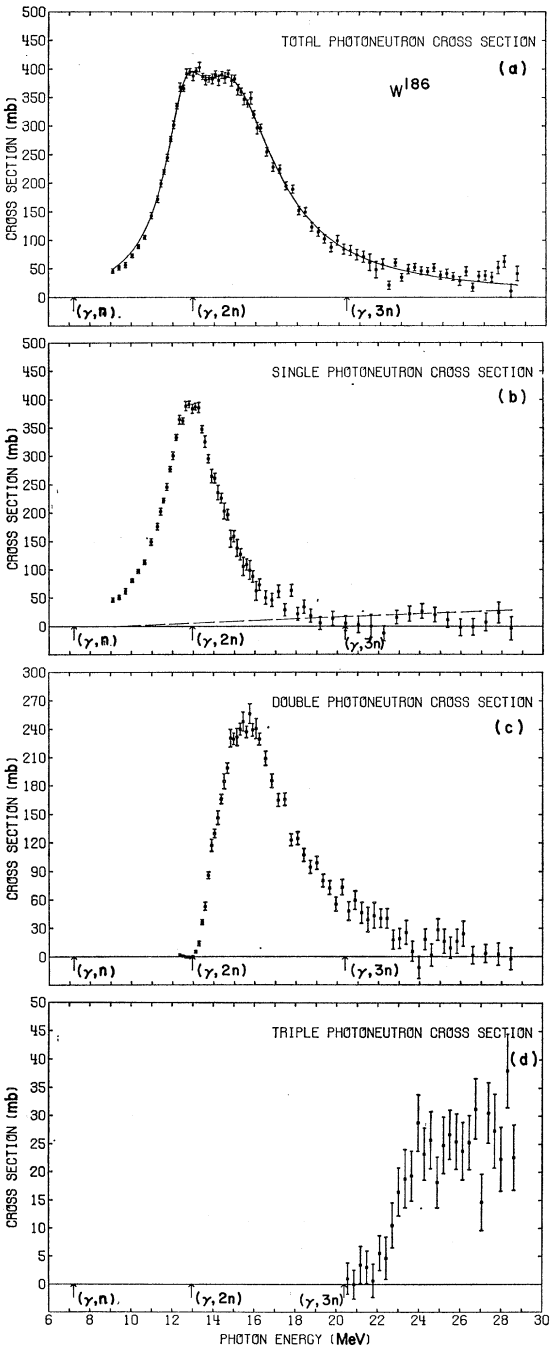

FIG. 8. Photoneutron cross sections for W^{186}: (a) $\sigma[(\gamma, n)+(\gamma, pn)+(\gamma, 2n)+(\gamma, p2n)+(\gamma, 3n)]$, (b) $\sigma[(\gamma, n)+(\gamma, pn)]$, (c) $\sigma[(\gamma, 2n)+(\gamma, p2n)]$, (d) $\sigma(\gamma, 3n)$.

of the region of deformed rare-earth nuclei. Again it is clear that the nucleus is prolate. There is some suggestion of structure just above threshold, and very definitely a broad hump, 2–3 MeV wide, centered at 24 MeV, which might also be indicated in the single-photoneutron cross section [Fig. 6(b)].

Carver and Turchinetz[12] measured the $Gd^{160}(\gamma, n)$ Gd^{159} cross section with bremsstrahlung and an activation technique, and obtained results in good agreement with those of Fig. 6(b). It is curious, however, that the low-lying location of the $(\gamma, 2n)$ threshold, together with the statistical behavior of the $(\gamma, 2n)$ cross section [see Fig. 6(c)] in taking over essentially the whole photon absorption cross section within about 3 MeV of this threshold, makes the *single*-photoneutron cross section look like a single-peaked giant resonance. This illustrates the crucial importance of performing properly the $(\gamma, 2n)$ cross-section measurements. Carver and Turchinetz, by looking at the (γ, n) process alone, did not, and were forced to come to the conclusion that their measurements showed no evidence for the splitting of the giant resonance in this most deformed of nuclei. The $(\gamma, 2n)$ cross section reaches its maximum value of about 175 mb at 16.2 MeV, and, as it should if the photoneutron emission process were completely statistical, decreases to a value consistent with zero at about 25.5 MeV, about 4 MeV above the $(\gamma, 3n)$ threshold. The $(\gamma, 3n)$ cross section [Fig. 6(d)] reaches its maximum value of about 20 mb at about 25.5 MeV, and then probably decreases somwhat.

3. Ho^{165}

The photoneutron cross sections for Ho^{165} were measured with far better statistics than the others reported upon here, partly because a large sample was available since holmium is monoisotopic, partly because there was no oxygen sample-blank subtraction to perform since a metal sample was used, and partly because considerably more time was alotted to the measurement since the results were essential to the proper interpretation of the measurements performed with the polarized holmium target described in Ref. 7. The total photoneutron cross section [Fig. 7(a)] again shows the double-humped giant resonance characteristic of prolate deformed nuclei. There is a definite shoulder in the cross section at about 9 MeV, and prominent structure well above the giant resonance at 24, 26, and 28 MeV. The single-photoneutron cross section [Fig. 7(b)] falls to small values by 19 MeV, about 5 MeV above the $(\gamma, 2n)$ threshold. The double-photoneutron cross section [Fig. 7(c)] reaches its maximum value of about 125 mb at 16.9 MeV, and decreases to small values by about 27 MeV, 4 MeV above the $(\gamma, 3n)$ threshold. Also, the statistical quality of the data is good enough to establish with confidence the sharp discontinuity in the slope of the $(\gamma, 2n)+(\gamma, p2n)$ cross section just below 20 MeV, near the $(\gamma, p2n)$ threshold [see also the ring-ratio data of Fig. 3(a)]. This phenomenon occurs as well for the other three nuclei studied here (and also in the Tb^{159} data of Ref. 10), but with less statistical certainty, and, for the cases of Gd^{160} and W^{186}, with the additional ambiguity introduced by the fact that the $(\gamma, 3n)$ thresholds for these last two nuclei occur at nearly the same energies as the $(\gamma, p2n)$ thresholds. Still, this suggests quite strongly that the $(\gamma, p2n)$ cross section cannot be neglected in a detailed treatment of the decay modes of the giant resonance. The $(\gamma, 3n)$ cross section [Fig. 7(d)] reaches its maximum value of about 16 mb at about 28.3 MeV, near the high-energy limit of the present measurement.

There have been several other photoneutron measurements on Ho^{165} reported previously. Welsh and Donahue[27] have measured the (γ, n) cross section at five discrete photon energies just above threshold; although their values below 9.5 MeV agree with the present data within experimental limits, their cross sections at 9.7 and 10.8 MeV are much higher. Hurst and Donahue,[25] using a similar technique, obtained slightly higher values at 9.0 and 9.7 MeV and a much lower value at 10.8 MeV than did Welsh and Donahue, but the last two values are still much higher than the present data. Thies and Spicer[15] measured both the neutron-yield cross section $\sigma[(\gamma, n)+(\gamma, pn)+2(\gamma, 2n)]$ and the activation cross section $\sigma(\gamma, n)$ with bremsstrahlung up to 18 MeV. Fuller and Hayward[16] measured the neutron-yield cross section up to 23 MeV, and corrected their data for the neutron multiplicity with a statistical computation. They later revised their absolute cross-section scale: their final results appear as Fig. 8 in Ref. 8. Axel *et al.*[17] performed a measurement very similar to the present one, using monoenergetic photons from positron annihilation up to 20 MeV and neutron-multiplicity counting. However, the efficiency of their neutron detector was only 8.1% (0.7% for double-photoneutron events), its variation with neutron energy was not taken into account, and their absolute cross-section uncertainty was 14% [18% for the $(\gamma, 2n)$ cross section].

The results of the giant-resonance experiments can be summarized by comparing the resonance parameters deduced from each, given in Table IV. The results of the older Livermore work on Ho^{165},[11] as well as the present results, are included for purposes of comparison. It is evident that, apart from the absolute cross-section scales, especially the one of Thies and Spicer,[15] there is good over-all agreement. Uncertainties have been attached to the values of Axel *et al.*[17] and to those for the present work in order to compare the two results in detail. It can be seen that some discrepancies remain outside the experimental limits, namely, in the values for $E_m(1)$, $E_m(2)$, and $\sigma_m(2)$. It is encouraging to note that on the important question of the magnitude and shape of the $(\gamma, 2n)$ cross section, the present data

[27] R. E. Welsh and D. J. Donahue, Phys. Rev. **121**, 880 (1961).

TABLE IV. Comparison with previous experiments on Ho^{165}.

Reference	$E_{\gamma\max}$ (MeV)	$E_m(1)$ (MeV)	$\sigma_m(1)$ (mb)	$\Gamma(1)$ (MeV)	$E_m(2)$ (MeV)	$\sigma_m(2)$ (mb)	$\Gamma(2)$ (MeV)
Thies and Spicer[a]	18	12.1	420	2.8	16.2	510	4.7
Fuller and Hayward[b]	23	12.2	219[b]	2.33	16	226[b]	≈5[b]
Axel *et al.*[c]	20	12.02[c] ±0.04	236[c] ±12	2.35[c] ±0.22	15.59[c] ±0.09	308[c] ±11	4.85[c] ±0.4
Bramblett *et al.*[d]	27	12.19[d]	200	2.65	15.87[d]	249	4.4
Present work	29	12.28 ±0.025	214 ±15	2.57 ±0.11	15.78 ±0.044	246 ±18	5.00 ±0.17

[a] Reference 15.
[b] References 8 and 16. Based on Ref. 8, the values for σ_m given in Ref. 16 were multiplied by 0.69. The value for $\Gamma(2)$ was estimated from the data.
[c] Reference 17. The values given here are the averages of the two sets of values given in Ref. 17, including their uncertainties. It is not clear how the very small uncertainties for the σ_m values were derived.
[d] Reference 11. The values for E_m given in Ref. 11 have been raised by about 0.7% in view of a more recent energy calibration accurate to ¼% instead of the older accuracy of 1%.

lie between the earlier data of Refs. 11 and 17. Still, the total cross section presented here agrees far better with the earlier Livermore work than with that of Ref. 17.

4. W^{186}

The total photoneutron cross section for W^{186} [Fig. 8(a)] shows the smallest splitting of the giant resonance of any of the nuclei reported on here, although that splitting is clearly present, and Lorentz-curve fitting shows that the higher-lying component has by far the larger area. The present measurements (in this case only) did not extend down to the (γ, n) threshold. No structure in the cross section above the giant resonance is clearly delineated, although there is some slight indication of a broad hump centered at about 24.5 MeV. The single-photoneutron cross section for W^{186} [Fig. 8(b)], even more so than for Gd^{160}, looks like a single-peaked giant resonance. Again, this phenomenon owes its origin to the low $(\gamma, 2n)$ threshold, and again, the only previous measurement of a photoneutron cross section (the bremsstrahlung-and-activation experiment of Carver *et al.*[13]) failed, for this reason, to illustrate the splitting of the giant resonance. (Also, the absolute cross section given in Ref. 13 is more than twice as large as the present data.) The single-photoneutron cross section decreases to a value consistent with zero by 19 MeV, 6 MeV above the $(\gamma, 2n)$ threshold, but becomes positive again for a 2–3-MeV region around 24.5 MeV, perhaps resulting from the (γ, pn) reaction. The $(\gamma, 2n)$ cross section for W^{186} [see Fig. 8(c)] is the largest ever measured, except for U^{235},[28] reaching a maximum value of about 250 mb at 15.7 MeV. This, too, results from the fact that W^{186} is a very neutron-rich isotope ($N=112$), so that the $(\gamma, 2n)$ process has a very low threshold (less than 13 MeV) and consequently contains most of the strength in the higher-energy peak of the giant resonance. The double-photoneutron cross section decreases to small values above 24 MeV, about 4 MeV above the $(\gamma, 3n)$ threshold, although it might contain a contribution from the $(\gamma, p2n)$ process at around 26 MeV. The $(\gamma, 3n)$ cross section [Fig. 8(d)] reaches its maximum value of about 30 mb at about 27.5 MeV, near the high-energy limit of the present measurement.

TABLE V. Parameters of Lorentz-curve fits to the giant resonance.

Nucleus	$E_m(1)$ (MeV)	$\sigma_m(1)$ [a] (mb)	$\Gamma(1)$ (MeV)	$E_m(2)$ (MeV)	$\sigma_m(2)$ [a] (mb)	$\Gamma(2)$ (MeV)
Eu^{153}	12.33±0.06	155±9	2.75±0.26	15.79±0.10	222±6	5.83±0.30
Tb^{159} [b]	12.22±0.04	181±6	2.64±0.16	15.67±0.06	220±4	4.97±0.19
Gd^{160}	12.23±0.06	215±9	2.77±0.25	15.96±0.09	233±6	5.28±0.30
Ho^{165}	12.28±0.02	214±5	2.57±0.11	15.78±0.04	246±3	5.00±0.17
Ta^{181} [c]	12.59±0.03	171±8	1.94±0.12	15.13±0.12	265±6	4.98±0.23
W^{186}	12.59±0.03	211±14	2.29±0.14	14.88±0.08	334±8	5.18±0.14

[a] The uncertainties for σ_m given here are relative. The absolute uncertainty is 7% (10% for Tb^{159} and Ta^{181}).
[b] The data of Ref. 10 were reanalyzed to obtain the values given in this and subsequent tables (see text).
[c] The data of Ref. 11 were reanalyzed to obtain the values given in this and subsequent tables (see text).

[28] C. D. Bowman, G. F. Auchampaugh, and S. C. Fultz, Phys. Rev. **133**, B676 (1964).

IV. DISCUSSION

A. Giant-Resonance Parameters

The classic collective description of the giant dipole resonance predicts that the total photon absorption cross section $\sigma(E_\gamma)$ for deformed nuclei is characterized as the sum of two Lorentz-shaped curves,

$$\sigma(E_\gamma)=\sum_{i=1}^{2}\left\{\sigma_m(i)\Big/1+\frac{[E_\gamma^2-E_m^2(i)]^2}{E_\gamma^2\Gamma^2(i)}\right\}, \quad (6)$$

where all quantities have been defined in Sec. I. For medium-heavy nuclei the Coulomb barrier greatly inhibits the emission of charged particles at giant-resonance energies, and the photon scattering cross section is always small above the (γ, n) threshold; thus, the total photoneutron cross section is an excellent approximation to the total photon absorption cross section. Therefore, the total photoneutron cross sections presented in Sec. III are fitted with two-component Lorentz curves. The fitting interval used for all four nuclei was 10.8–18.8 MeV; reasonable departures from this interval do not change the results noticeably.[7,18,19] The χ^2 values for these fits are 2.21, 1.34, 1.62, and 0.90 for Eu^{153}, Gd^{160}, Ho^{165}, and W^{186}, respectively. The parameters of these Lorentz-curve fits, plotted in Figs. 5(a), 6(a), 7(a), and 8(a), are given in Table V. The Lorentz parameters for Tb^{159} and Ta^{181} from the older work done at this laboratory also are given in Table V. The differences in the parameters from the values given in Refs. 10 and 11 came about from (1) a slight energy shift (the data points move up in energy about 0.7%) in accordance with a more recent determination of the energy scale (the old scale was stated to be accurate to only 1%), and (2) reanalysis of the Lorentz-curve fitting procedure so that the fitting interval is 10.8–18.8 MeV, in order that it be the same as for the other nuclei presented here. Also, owing to the relatively poorer statistical quality of the Ta^{181} data, the number of fitting parameters was reduced from six to five. The means by which this was done was to fix the value of β (see below and Table VI) to equal the average for the other five nuclei, namely, 34.0±0.2 MeV; this fixes the mean resonance energy E_m (defined in Table VI) to equal 14.28±0.12 MeV. This procedure was judged to be the least model-dependent of any; in particular, it has a minimal effect on the nuclear eccentricity. The χ^2 values for these fits are 1.00 and 0.57 for Tb^{159} and Ta^{181}, respectively. These χ^2 values are very low, of course, mainly because the data of Refs. 10 and 11 have larger statistical uncertainties than the present data, and consequently are fitted more easily. For the case of Ta^{181} in particular, this implies that the Lorentz parameters given in Table V should be accepted with some reservation, pending the availability of better data.

Values of the parameters for the classical theories are given in Table VI. These include α and β, the proportionality constants characterizing the variation of the mean resonance energy E_m with mass number; and K, the nuclear symmetry energy computed from Eq. (5). The mass range of the present measurements is not sufficiently wide to choose between the competing collective theories[1,2] which predict the $A^{-1/3}$ and $A^{-1/6}$ dependence of E_m: both α and β are nearly constant here, although β appears to vary slightly less than α. The values for the nuclear symmetry energy K given in Table VI agree well with the values for other medium-heavy and heavy nuclei measured at this Laboratory, listed in Ref. 23.

TABLE VI. Parameters for classical theories.[a]

Nucleus	E_m [b]	α [c]	β [d]	K [e]
Eu^{153}	14.64±0.08	78.3±0.4	33.8±0.2	25.9±0.7
Tb^{159}	14.52±0.05	78.7±0.3	33.8±0.1	26.2±0.4
Gd^{160}	14.72±0.07	79.9±0.4	34.3±0.2	27.3±0.7
Ho^{165}	14.62±0.03	80.2±0.2	34.2±0.1	27.2±0.3
Ta^{181}	14.28±0.12	80.8±0.7	34.0±0.2 [f]	27.3±1.0
W^{186}	14.12±0.06	80.5±0.3	33.7±0.1	27.3±0.4

[a] All quantities in this table are given in MeV.
[b] E_m is the mean energy of the giant resonance, defined as $E_m=\frac{1}{3}[E_m(1)+2E_m(2)]$ for prolate nuclei.
[c] The hydrodynamic parameter α is defined by $E_m=\alpha A^{-1/3}$.
[d] The collective parameter β is defined by $E_m=\beta A^{-1/6}$.
[e] The nuclear symmetry energy K is computed from Eq. (5) in the text.
[f] This value was chosen as an input parameter for further analysis, and was not derived from the data (see text).

Values for various nuclear shape parameters, computed from the Lorentz parameters of Table V, are given in Table VII. These are R_A, the area ratio defined by Eq. (4), and predicted to be one-half for prolate nuclei; η, the deformation parameter defined by Eq. (1); ϵ, the nuclear eccentricity defined by Eq. (2); the deformation parameter β_2 used by Stelson and Grodzins,[29] defined by the relation

$$\beta_2=[(5\pi)^{1/2}/3](Q_0/ZR^2)=\tfrac{2}{3}(\pi/5)^{1/2}\epsilon\approx 0.53\epsilon; \quad (7)$$

and δ, the deformation parameter of Nilsson,[30] defined by

$$Q_0\approx\tfrac{4}{5}ZR^2\delta(1+\tfrac{2}{3}\delta) \quad (8)$$

from which

$$\delta\approx\tfrac{1}{4}[(12\epsilon+9)^{1/2}-3]. \quad (9)$$

It can be shown that for the range of deformations for the nuclei studied here, the four parameters η, ϵ, β_2, and δ are very nearly completely equivalent in describing the deformation; therefore, only one of them, namely, ϵ, will be used for further analysis. This present definition of the nuclear eccentricity also can be expressed as

$$\epsilon=(b^2-a^2)/R^2, \quad (10)$$

[29] P. H. Stelson and L. Grodzins, Nucl. Data **A1**, 21 (1965).
[30] S. G. Nilsson, Kgl. Danske Videnskab. Selskab, Mat.-Fys. Medd. **29**, No. 16 (1955).

TABLE VII. Nuclear shape parameters.

Nucleus	R_A [a]	η [b]	ϵ [c]	β_2 [d]	δ [e]
Eu^{153}	0.330±0.076	1.308±0.016	0.595±0.015	0.315±0.008	0.254±0.006
Tb^{159}	0.437±0.066	1.310±0.010	0.598±0.009	0.316±0.005	0.255±0.003
Gd^{160}	0.484±0.104	1.335±0.015	0.645±0.014	0.341±0.007	0.273±0.005
Ho^{165}	0.447±0.050	1.313±0.006	0.604±0.006	0.319±0.003	0.258±0.002
Ta^{181}	0.251±0.045	1.222±0.014	0.433±0.010	0.229±0.005	0.193±0.004
W^{186}	0.279±0.048	1.200±0.010	0.390±0.006	0.206±0.003	0.174±0.002

[a] The ratio of the areas under the two Lorentz components of the giant resonance, R_A is defined by Eq. (4) in the text.
[b] The deformation parameter η is computed from Eq. (1) in the text.
[c] The nuclear eccentricity ϵ is computed from Eq. (2) in the text.
[d] The deformation parameter of Ref. 29, β_2 is defined by Eq. (7) in the text.
[e] The deformation parameter of Ref. 30, δ is defined by Eq. (9) in the text.

where b and a are the semimajor and semiminor axes, respectively, and R is the radius of a sphere of equal volume; for a prolate spheriod,

$$R^3=a^2b. \tag{11}$$

The area-ratio (R_A) values given in Table VII show a wide variation as one moves across the region of deformed nuclei, and thus illustrate what is perhaps the most obvious breakdown of the simple hydrodynamic theory. To test this breakdown further, the total neutron cross sections also were fitted with Lorentz curves in the same way as before, but this time constrained to give $R_A=\frac{1}{2}$. The new χ^2 values which result from this procedure give a further indication of the breakdown of the simple theory. They are 5.11, 1.85, 1.36, 9.21, and 1.12 for Eu^{153}, Tb^{159}, Gd^{160}, Ho^{165}, and Ta^{181}, respectively; no reasonable fit to the W^{186} data could be obtained under this constraint. Only the χ^2 value for Gd^{160}, for which R_A already was nearly 0.5 ($R_A=0.484$), is close to that for the free fit; the remainder are about a factor of 2 or more higher. These values for R_A are plotted versus neutron number N in Fig. 9 along with the values for ϵ and Q_0 deduced from the present data. The values for Q_0 in Fig. 9 were computed for a nuclear radius parameter $R_0=1.26\,F$ (see below). One can see immediately the correspondence between R_A and the shape parameters; thus, not only does the departure of R_A from $\frac{1}{2}$ illustrate the breakdown of the simple hydrodynamic theory, but it also shows that that theory is best for large static deformations. This is in contrast to the single-particle model of Wilkinson,[31] which gives its best answers for spherical nuclei, and departs most from experiment at large deformations. This is apparent from a glance at Fig. 7 of Ref. 31, in which the theoretical giant-resonance width versus atomic weight is plotted. The total widths measured here (all about 6–8 MeV, as can be seen from Figs. 5–8 and Refs. 10 and 11) all are smaller than the predictions of Ref. 31, but particularly so for Tb^{159}, Gd^{160}, and Ho^{165}, the most deformed nuclei. Wilkinson recognized at the time that this was likely to be case; but the situation has not been corrected since that time, partly owing to the computational difficulties involved. Incidentally, these determinations of the total widths depend critically upon an accurate measurement of the photon absorption cross section on the high-energy side of the giant resonance. The cross section in this region is very difficult to measure with bremsstrahlung, since the uncertainties inherent in any unfolding technique are largest here; likewise, a knowledge of the $(\gamma, 2n)$ cross section here is vital. It also should be pointed out that the value of R_A for As^{75} (from Ref. 19) is 0.24, which shows that the hydrodynamic model also fails for

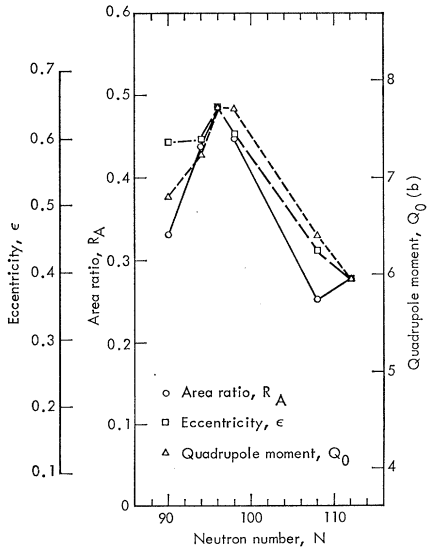

FIG. 9. The area ratio R_A, nuclear eccentricity ϵ, and intrinsic quadrupole moment Q_0 plotted versus neutron number N. The data were scaled between the value for Gd^{160} and that for W^{186}. The absolute scale for Q_0 is based on a mean radius parameter $R_0=1.26$ F. The lines merely connect the three sets of data points. The experimental uncertainties have been omitted for clarity but are given in Tables VII and VIII; their average values are 0.065 (17%) for R_A, 0.010 (1.9%) for ϵ, and 0.26b (3.7%) for Q_0.

[31] D. H. Wilkinson, Phil. Mag. 3, 567 (1958).

TABLE VIII. Nuclear radius parameters.

Nucleus	Q_0 [a] (b)	Refs.	ϵ [b]	R_0 [c] (F)	Q_0 [d] (b)
Eu^{153}	6.99±0.08	e, f	0.595±0.015	1.276±0.018	6.80±0.28
Tb^{159}	7.41±0.11	e	0.598±0.009	1.274±0.013	7.23±0.26
Gd^{160}	7.55±0.17	g	0.645±0.014	1.245±0.020	7.71±0.30
Ho^{165}	7.56±0.11	e	0.604±0.006	1.246±0.011	7.71±0.26
Ta^{181}	6.89±0.21	h, i	0.433±0.010	1.306±0.025	6.43±0.26
W^{186}	5.96±0.05	g, j, k	0.390±0.006	1.259±0.011	5.96±0.21

[a] Values taken from or computed from the references listed in column 3.
[b] Values from present data (Table VII).
[c] Computed from Eq. (2) in the text.
[d] The "best" values for Q_0 deduced from the present data, computed from Eq. (2) in the text, taking R_0 to be 1.26±0.02 F.
[e] M. C. Oleson and B. Elbek, Nucl. Phys. **15**, 134 (1960).
[f] R. A. Carrigan, Jr., P. D. Gupta, R. B. Sutton, M. N. Suzuki, A. C. Thompson, R. E. Coté, W. V. Prestwich, A. K. Gaigalas, and S. Raboy, Phys. Rev. Letters **20**, 874 (1968).
[g] P. H. Stelson and L. Grodzins, Nucl. Data *A1*, 21 (1965).
[h] F. K. McGowan and P. H. Stelson, Phys. Rev. **109**, 901 (1958).
[i] E. M. Bernstein and R. Graetzer, Phys. Rev. **119**, 1321 (1960).
[j] R. C. Barrett, S. Bernow, S. Devons, I. Duerdoth, D. Hitlin, J. W. Kast, W. Y. Lee, E. R. Macagno, J. Rainwater, and C. S. Wu, Columbia University Pegram Nuclear Physics Lab. Report No. NYO-72-191, 1968, p. 74 (unpublished).
[k] R. G. Stokstad and B. Persson, Phys. Rev. **170**, 1072 (1968).

this case of a nucleus whose equilibrium configuration probably is spherical, but whose vibrational deformation is large (its average eccentricity is 0.37).

It can be seen from the uncertainties of the E_m values in Table V that by far the largest uncertainty in the determination of Q_0 from Eq. (2) is that in the value used for R_0. Since R_0 is known currently for these nuclei to no better than 5%, then to such values of Q_0 must be associated an uncertainty of no less than 10%, far in excess of the present uncertainty in the values for ϵ (the worst case is that of Eu^{153}, for which the uncertainty in ϵ is 2.5%). This is the reverse of the situation that exists for Coulomb-excitation measurements, where the $B(E2)$ values give Q_0 directly, but a value for the deformation involves an assumption for R_0. Thus, the combination of the two kinds of measurements provides a new determination of the mean radius parameter for these nuclei, with a considerably greater accuracy than has been achieved heretofore. The best available data for Q_0 from Coulomb-excitation experiments (together with two values obtained from μ-mesic x-ray studies), weighted appropriately, are given in the second column of Table VIII. These values, together with the measured eccentricities (listed again in column 4 of Table VIII), have been used to compute values for R_0 from Eq. (2). These new values for R_0 are listed in column 5 of Table VIII; their weighted average is 1.26±0.02 F. One observes (except for the case of Ta^{181}) that there is no systematic trend in these values for R_0; therefore, this average value can be considered to be typical of nuclei in this region of the periodic table. Now, meaningful values for Q_0 can be computed from the present data, using Eq. (2) and this value for R_0; these are given in the last column of Table VIII. Of the Q_0 values thus obtained, only that for Ta^{181} does not agree well with the best data published previously. Perhaps this results in part from

TABLE IX. Integrated cross sections.

Nucleus	$E_{\gamma\,\max}$ (MeV)	$\sigma_{\rm int}[(\gamma,n)+(\gamma,pn)]$ [a] (MeV-b)	$\sigma_{\rm int}[(\gamma,2n)+(\gamma,p2n)]$ [a] (MeV-b)	$\sigma_{\rm int}(\gamma,3n)$ [a] (MeV-b)	$\dfrac{\sigma_{\rm int}[(\gamma,2n)+(\gamma,p2n)]}{\sigma_{\rm int}(\gamma,\text{total})}$ [b]	$\frac{1}{2}\pi[\sigma_m(1)\Gamma(1)+\sigma_m(2)\Gamma(2)]$ [c] (MeV-b)	$0.06\,NZ/A$ (MeV-b)
Eu^{153}	28.9	1.57	0.67	0.04	0.29±0.04	2.70±0.19	2.22
Tb^{159}	28.0	1.41	0.89	d	0.39±0.08	2.47±0.12	2.31
Gd^{160}	29.5	1.45	1.00	0.08	0.39±0.05	2.87±0.20	2.30
Ho^{165}	28.9	1.73	0.74	0.04	0.29±0.04	2.80±0.09	2.39
Ta^{181}	24.6	1.31	0.88 [e]	f	0.40 [e]±0.08	2.59±0.15	2.61
W^{186}	28.6	1.66	1.19	0.15	0.40±0.05	3.47±0.17	2.67

[a] All measured integrated cross-section values are given for an energy region from threshold to $E_{\gamma\,\max}$.
[b] The word "total" in this table refers to the total photoneutron cross section, $\sigma[(\gamma,n)+(\gamma,pn)+(\gamma,2n)+(\gamma,p2n)+(\gamma,3n)]$.
[c] The uncertainties listed here are relative; to get the absolute uncertainty, a systematic uncertainty of 7% (10% for Tb^{159} and Ta^{181}) must be folded into the values for σ_m.
[d] Not measured in Ref. 10; $\sigma_{\rm int}[(\gamma,2n)+(\gamma,p2n)]$ contains $\frac{3}{2}\sigma_{\rm int}(\gamma,3n)$.
[e] Because $E_{\gamma\,\max}$ is so low, these values cannot be compared to the rest.
[f] Not measured in Ref. 11; the $(\gamma,3n)$ cross section below 24.6 is MeV probably negligible.

TABLE X. Integrated moments[a] of the measured photoneutron cross section and sum rules.

Nucleus	σ_{-1} (mb)	$\sigma_{-1}A^{-4/3}$ (mb)	σ_{-2} (mb-MeV^{-1})	$\frac{\sigma_{-2}}{0.00225\ A^{5/3}}$	$\frac{\sigma_{-2}K}{0.05175\ A^{5/3}}$	$\frac{0.05175\ A^{5/3}}{\sigma_{-2}}$ (MeV)
Eu^{153}	148	0.181	10.18	1.03	1.16±0.11	22.2±1.6
Tb^{159}	151	0.175	10.49	1.00	1.14±0.13	23.0±2.3
Gd^{160}	169	0.195	12.09	1.14	1.35±0.13	20.2±1.4
Ho^{165}	166	0.183	11.56	1.04	1.23±0.10	22.2±1.6
Ta^{181} [b]	(149)	(0.145)	(10.66)	(0.82)	(0.97±0.13)	(28.1±2.8)
W^{186}	203	0.191	14.51	1.06	1.26±0.11	21.6±1.5

[a] $\sigma_{-1}=\int_{E\text{thr}}^{E\gamma\,\max}\sigma E^{-1}\,dE$ and $\sigma_{-2}=\int_{E\text{thr}}^{E\gamma\,\max}\sigma E^{-2}\,dE$, where σ is the total photoneutron cross section.

[b] Because $E_{\gamma\,\max}$ is so low, the values for Ta^{181} cannot be compared to the rest.

the fact that the Coulomb-excitation measurements on Ta^{181} are the oldest and have the largest uncertainties of any of those cited here, but perhaps it can be ascribed in part to the relatively poorer quality of the earlier photoneutron data of Ref. 11. In fact, the results of an early electron-scattering experiment of Hofstadter[32] indicate that R_0 for Ta^{181} is about 1.25 F, in agreement with the average R_0 obtained here. More electron-scattering data in this region of the periodic table would be valuable; unfortunately, the only other measurement reported to date is that of Safrata *et al.*,[33] who obtain a value of R_0 of 1.23 F for Ho^{165}.

It must be emphasized, however, that this analysis leans very heavily on the classical model, which now is known to break down in several respects.[7] For instance, the prediction that $R_A=\frac{1}{2}$ depends upon the TRK sum rule being independent of the nuclear orientation (and hence of the nuclear radius); a proper quantum-mechanical description based on a reasonable radial wave function might not require this condition. An alternative approach is to compute the nuclear deformation from the quadrupole moments measured by Coulomb excitation using the more conventional mean radius parameter of 1.20 F, and then to ascribe the discrepancy with the present data that results from this procedure to the existence of higher-order even static multipole moments. Indeed, the α-particle-scattering measurements of Hendrie *et al.*[34] show that the quadrupole deformations β_2 of a variety of deformed nuclei are appreciably lower than those derived in this way from the Coulomb-excitation data, and thus demonstrate that the higher-multipole deformations β_4 (and β_6) contribute appreciably to the measured Q_0 values. Furthermore, the data of Ref. 34 show that the nuclei which have large absolute β_4 values occur near the limits of the region of deformed nuclei, where the classical prediction for R_A breaks down most noticeably; for the most deformed nuclei, where the classical theory is best, the values of β_4 are nearly zero. To be sure, these higher moments might influence the shape of the giant resonance as well. However, until more detailed theoretical calculations become available, one only can hope that the discrepancies between the Q_0 values measured by Coulomb excitation, which depend on the nuclear charge distribution, and the β_2 (or ϵ) values measured here (or by α-particle scattering), which depend on the nuclear matter distribution, can be resolved in this way.

B. Integrated Cross Sections

The integrated cross sections measured in this work are summarized in Table IX. Columns 3, 4, and 5 in the table list the integrated single-, double-, and triple-photoneutron cross sections, respectively; column 6 lists the ratio of the integrated double to total photoneutron cross sections; column 7 lists the total area under the Lorentz-curve fits to the total photoneutron cross sections, which are to be compared with the TRK sum-rule predictions given in the last column. The ratios of the values in column 7 to those in column 8 range from 0.97 (for Ta^{181}) to 1.30 (for W^{186}), and average 1.16±0.07. These ratios indicate the maximum amount of exchange-force enhancement of the dipole sum-rule values that might be needed to account for the giant resonance, and are consistent with many measurements on other nuclei made previously at this laboratory.

The integrated moments of the measured total photoneutron cross sections σ_{-1} and σ_{-2} are given in columns 2 and 4, respectively, of Table X. Migdal[35] derived a sum rule for σ_{-2} based on the assumption of a constant nuclear (but variable neutron and proton) density, similar to the approach used subsequently by Steinwedel and Jensen.[2] The value of σ_{-2}, which is

[32] R. Hofstadter, Ann. Rev. Nucl. Sci. **7**, 231 (1957).

[33] R. S. Safrata, J. S. McCarthy, W. A. Little, M. R. Yearian, and R. Hofstadter, Phys. Rev. Letters **18**, 667 (1967).

[34] D. L. Hendrie, N. K. Glendenning, B. G. Harvey, O. N. Jarvis, H. H. Duhm, J. Saudinos, and J. Mahoney, Phys. Letters **26B**, 127 (1968).

[35] A. Migdal, Zh. Eksperm. i Teor. Fiz. **15**, 81 (1945).

proportional to the nuclear polarizability, is predicted to be[36]

$$\sigma_{-2}=0.05175A^{5/3}/K \text{ mb-MeV}^{-1} \qquad (12)$$

for spherical nuclei, where K is in MeV and $R_0=1.20$ F; for $K=23$ MeV, $\sigma_{-2}=0.00225A^{5/3}$ mb-MeV^{-1}. It can be seen from column 5 of Table X that the experimental values lie within 14% of this prediction, and four of the five values (because $E_{\gamma\max}$ was so low for the Ta^{181} experiment, that result cannot be used) lie within 6% of it. This can be taken as an indication that 23 MeV is a reasonable value for the coefficient of the volume-symmetry–energy term in the semiempirical mass formula, for spherical nuclei of equal volume. If instead of the constant 23 MeV, however, one uses the values for K given in Table VI, column 6 in Table X shows that the agreement in this case is not nearly so good. Indeed, the values of the nuclear symmetry energy computed from the values for σ_{-2} by use of Eq. (12), listed in the last column of Table X differ from those in Table VI by an average of 23%, and thus show that there is a serious discrepancy between the two methods of computing the nuclear symmetry energy from the data. Since this does not appear to be the case for nuclei which have no equilibrium deformation,[18,19,37] where the two methods yield essentially the same results, one might assume the difference to have its origin in the nuclear deformation; and since the deformation is a surface phenomenon, one then can ascribe this difference to the existence of a surface-symmetry–energy contribution (measured quantitatively in the present experiment) to the total (mostly volume) symmetry energy. Consequently, it is clear that the approach of Levinger[36] and Migdal[35] need not be valid for nonspherical nuclei, where the nuclear density at the nuclear surface is a strong function of orientation. Further theoretical work now is needed to put this suggestion on a quantitative basis.

C. Nuclear Level Densities

The ratio of the $(\gamma, 2n)$ to the total photoneutron cross section for a few MeV above the $(\gamma, 2n)$ threshold in the target nucleus gives the nuclear level density in the nucleus having one neutron less than the target nucleus at the appropriate excitation energy $U=E_\gamma-E_{\text{thr}}(\gamma, n)-E_n-\Delta$, where E_γ and E_n are the photon and neutron energies, respectively, $E_{\text{thr}}(\gamma, n)$ is the (γ, n) threshold, and Δ is a correction to the ground state of the target-minus-one-neutron nucleus from shell and pairing effects. As in Refs. 18 and 19, the present data have been analyzed with the use of two formulae for the density of states $\rho(a, U)$, suggested by Ericson[38] and by Blatt and Weisskopf,[39] where a is the nuclear level density parameter. A parameter search was conducted for a and Δ, using a least-squares fitting technique for the ratio $\sigma(\gamma, 2n)/\sigma(\gamma, \text{total})$ in the photon energy range between the $(\gamma, 2n)$ threshold and the point where the scatter and uncertainty in the data dictate that the fit to this cross section ratio could not be improved further. In practice, this procedure gives a family of curves corresponding to pairs of values for a and Δ, all of which have approximately the same χ^2 values. In order to choose the correct pair, the average neutron energy $\bar{E}_n$ of the first neutron emitted from the target nucleus was computed for each fit; the correct one then is chosen by comparing the calculated $\bar{E}_n$ with the measured $\bar{E}_n(1)$ from the ring-ratio data. For example, Fig. 10 shows the ratio of the $(\gamma, 2n)$ cross section to the total photoneutron cross section for Eu^{153}, plotted as a function of photon energy. The solid line is the theoretical fit for $a=5.4$ MeV^{-1} and $\Delta=1.0$ MeV when the Ericson[38] formula for the density of states is used. These values for a and Δ give the value of $\bar{E}_n=1.43$ MeV for photon energy $E_\gamma=E_m(1)=12.33$ MeV, in agreement with the ring-ratio value for $\bar{E}_n(1)$ given in Table III.

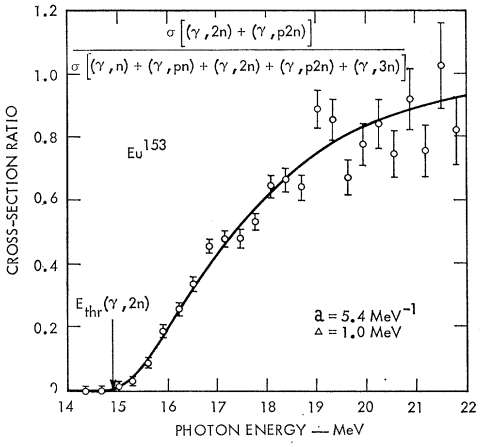

FIG. 10. Ratio of the double to the total photoneutron cross section for Eu^{153}. The solid line is derived from the theoretical expression for the nuclear density of states given in Ref. 38, evaluated for a level-density parameter $a=5.4$ MeV^{-1}, and including a shell-plus-pairing-effect parameter $\Delta=1.0$ MeV.

The results of this anlysis are given in Table XI. The lower and upper limits of the range of excitation energy, denoted by $U_<$ and $U_>$, respectively, are given in columns 2 and 3 of the table, and refer to the target-minus-one neutron nucleus with no shift of its ground state for shell and pairing effects (i.e., $\Delta=0$). Column 4 and 7 list the values for a when $\Delta=0$, and the other columns list the best pair of values for a and Δ, which were computed as described above. Since there are no

[36] J. Levinger, *Nuclear Photo-Disintegration* (Oxford University Press, London, 1960), p. 51.

[37] S. C. Fultz, B. L. Berman, R. L. Bramblett, J. T. Caldwell, and M. A. Kelly, Bull. Am. Phys. Soc. **13**, 35 (1968); University of California Lawrence Radiation Laboratory Report No. UCRL-71512, 1968 Phys. Rev. (to be published).

[38] T. E. Ericson, Advan. Phys. **9**, 425 (1960).

[39] J. M. Blatt and V. F. Weisskopf, *Theoretical Nuclear Physics* (John Wiley & Sons, Inc., New York, 1952), p. 379.

TABLE XI. Nuclear level density parameters.

Nucleus	$U_<$ [a] (MeV)	$U_>$ [b] (MeV)	From Ericson formula[c] $a(0)$ (MeV^{-1})	Δ (MeV)	$a(\Delta)$ (MeV^{-1})	From Blatt and Weisskopf formula[d] $a(0)$ (MeV^{-1})	Δ (MeV)	$a(\Delta)$ (MeV^{-1})
Eu^{152}	6.3	13.3	5.8	1.0	5.4	2.3	1.1	1.8
Tb^{158}	6.8	13.7	12.7	$\sim$0 [e]	($\sim$12.7)	7.7	$\sim$0 [e]	($\sim$7.7)
Gd^{159}	6.0	12.9	9.3	0.7	8.8	4.6	1.0	3.7
Ho^{164}	6.6	13.5	6.9	1.6	6.1	3.1	1.7	2.0
Ta^{180}	6.8	14.3	18.2	$\sim$1 [e]	($\sim$16.4)	12.0	$\sim$1 [e]	($\sim$10.2)
W^{185}	5.8	12.4	10.1	2.5	7.9	5.2	2.6	2.3

[a] $U_< = E_{\rm thr}(\gamma, 2n) - E_{\rm thr}(\gamma, n)$.
[b] $U_> = E_{\gamma\,\rm max} - E_{\rm thr}(\gamma, n)$.
[c] $\rho \propto U^{-2} \exp[2(aU)^{1/2}]$.
[d] $\rho \propto \exp[2(aU)^{1/2}]$.
[e] Since there are no ring-ratio data for these two nuclei, the Δ values were estimated from the χ^2 values alone (see text).

ring-ratio data for the cases of Tb^{158} and Ta^{180}, however, the best pair of a and Δ values was estimated from the slowly-varying χ^2 values alone. The values chosen (and listed in Table XI) correspond to $\bar{E}_n(1)|_m$ values of 1.8 and 1.7 MeV for Tb^{159} and Ta^{181}, respectively, in reasonable agreement with the rest of the values given in Table III. Again, as was found in previous cases,[18,19] although the values for a might differ greatly, depending on which formula for the density of states was used, the values for Δ are consistent, and therefore one can attach some validity to this determination of the influence of shell and pairing effects on the nuclear level density. In the case of three of the four nuclei studied here, namely, Eu^{152}, Gd^{159}, and Ho^{164}, it is reasonable to attribute essentially all of the effective ground-state shift Δ to pairing effects, since the neutron configurations of all three lie nowhere near closed neutron shells. (This is undoubtedly the case for Tb^{158} and Ta^{180} as well.) However, since the Δ value for W^{185} (2.5 MeV) is somewhat higher than the others, perhaps one can attribute this to the fact that W^{185} lies closer than the other nuclei studied here both to neutron and to proton closed shells. Lastly, it should be pointed out that the a values obtained here are considerably lower than those obtained with other experimental techniques. For instance, Owens and Towle,[40] using neutron inelastic scattering, obtain a values in the region of deformed rare-earth nuclei which average about 15, or $A/12$, using the Ericson density of states formula for excitation energies U ranging from 2.5 to 6.5 MeV. Possibly the present average of 10 for the corresponding a values results from the fact that the present results apply for a range of U from 6.5 to 13.5 MeV, but the discrepancy seems far too large to be explained in this way.

ACKNOWLEDGMENTS

The authors wish to thank S. Dietrich for help in the data analysis, Miss C. Hunt for computer programming, E. Dante and the other members of the accelerator staff, and Dr. A. K. Kerman, Dr. M. S. Weiss, Dr. A. Goldberg, and Dr. P. F. Yergin for several valuable discussions.

[40] R. O. Owens and J. H. Towle, Nucl. Phys. **A112**, 337 (1968).